Journal of Crystal Growth 449 (2016) 156–162

Contents lists available at ScienceDirect

Journal of Crystal Growth

journal homepage: www.elsevier.com/locate/jcrysgro

Controlled Cu nanoparticle growth on wrinkle affecting deposition of large scale graphene

Mohsin Ahmed [a,*], Md Jasim Uddin [b], Muhammad Anisur Rahman [c], Naoki Kishi [a], Tetsuo Soga [a]

[a] Department of Frontier Materials, Nagoya Institute of Technology, Nagoya, Japan
[b] School of Electrical Engineering and Computer Science (EECS), Queensland University of Technology, Brisbane, QLD 4111, Australia
[c] Monash University, Mechanical and Aerospace Engineering, Clayton Campus, Melbourne, Victoria 3800, Australia

ARTICLE INFO

Article history:
Received 20 January 2016
Received in revised form
23 May 2016
Accepted 2 June 2016
Communicated by: Tatau Nishinaga
Available online 8 June 2016

Keywords:
Graphene
Chemical Vapor Deposition (CVD)
Cu nanoparticle

ABSTRACT

For Chemical Vapor Deposition (CVD) grown graphene on Cu substrate, deviation from atomic orientation in crystals may be resulted from diffusion of abnormalities in the form of Cu nanoparticle (NP) formation or defects and affects graphene quality and properties drastically. However, for the uniform graphene deposition, mechanism of nanoparticle formation and its suppression procedure need to be better understood. We report growth of graphene, affected by Cu nanoparticles (NPs) emergence on Cu substrates. In the current study, growth of these nanoparticles has been suppressed by fine tuning of carrier gas by two-fold gas insertion mechanism and hence, quality and uniformity of graphene is significantly improved. It has been also observed that during the deposition by CVD, Cu nanoparticles cluster preferentially on wrinkles or terrace of the Cu surface. Composition of NP is extensively studied and found to be the oxide nanoparticle of Cu. Our result, controlled NP growth affecting deposition of graphene layer would provide useful insight on the growth of uniform and high quality Single layer or bilayer graphene for numerous electronics applications.

1. Introduction

Graphene has fascinating electrical and mechanical properties. However, the beneficial features of graphene are not guaranteed unless continuous, high quality graphene is obtained. In graphene synthesis, grain boundaries and defects are crucial factors that cause disruption of electronic connectivity and structural continuity and hence contribute to low charge carrier mobility [1–4] and poor mechanical properties [5].

Graphene on transition metals by Chemical Vapor Deposition (CVD) method has been extensively studied [3,6–8] in recent times. Depositing graphene on Cu has many beneficial aspects, resulting from low carbon solubility [9,10] and self-limiting diffusion criteria [11] of Cu and consequently, growth of large scale graphene has become feasible. Several techniques have been applied to grow continuous graphene by CVD; these are surface treatments like mechanical and chemical polishing [12] and oxygen treatment [6], suppression of nucleation [13,14], changing the gas proportions [15] and introducing a Cu–Ni alloy [16,17].

Recent advancement in CVD method has allowed large scale synthesis of single layer graphene on Cu [18,19]. To date, achieving large scale growth of bilayer graphene (BLG) by CVD has been extremely challenging. Most of the bilayer graphene are fabricated by mechanical exfoliation method, which have limited sizes and are certainly not scalable [20,21]. These limitations can be overcome a certain extent by CVD. However, presence of defects in CVD grown BLG compromises uniformity of graphene, affecting electronics performance significantly [22]. It is highly expected to produce single-crystal graphene with no or few defective sites and hence, avoid poor mechanical and electrical performance on exploited graphene. In CVD process, quality of graphene is greatly affected by morphology of copper surface such as wrinkles and impurity particles. During heating and cooling process by CVD, Cu foil shrinks and creates thermal stress and strain on the grown graphene and Cu and leave wrinkles as strain relaxation [23]. Gang et al. revealed the relation of wrinkle sites and graphene deposition on the copper surface and described wrinkles as nucleation seeds. Furthermore, copper nanoparticles have been depicted in few articles that affect nucleation for graphene growth [23–25]. In CVD process, the reaction between the copper substrate and the graphene creates a high level of hydrostatic compression to couple the graphene to the substrate [26]. During cooling period, the proportion of H_2 gas may affect the graphene growth and create

* Corresponding author. Present address: Environmental Future Research Institute, Griffith University, QLD, Australia.
E-mail address: mohsin.ahmed@griffithuni.edu.au (M. Ahmed).

http://dx.doi.org/10.1016/j.jcrysgro.2016.06.004
0022-0248/

exposed Cu near grain boundaries by reducing graphene. This exposed area comes in contact with oxygen or vapor and cause the creation of oxide nanoparticle of Copper [27]. Mondal et al. showed that these Cu nanoparticles enhance catalytic performance for graphene and graphite growth [28]. An analysis detailing nanoparticle growth has been provided by Gan et al. which reveals that nanoparticles can act as nucleation seeds for graphene growth [29]. However, an initiation, composition and key factors that affects formation of nanoparticles and how this nanoparticle relate to wrinkle is still unanswered.

Here, we report the growth of nanoparticle near the wrinkle or terrace of the Cu surface. Growth mechanism of Cu nanoparticles and the incumbent impact on the deposition of a continuous graphene layer by CVD process is revealed in this study. We propose the creation of Cu nanoparticles as an outcome of wrinkle formation and gas kinetics in the CVD process. Our observations may contribute to the growth of large scale monolayer or bilayer of graphene on the metal surface.

2. Experimental details

Polycrystalline Cu foil, purchased from Nilaco Corporation of 99% purity and 25 μm thickness was cut into 5 mm × 5 mm pieces. A 120 cm long and 75 mm diameter quartz tube was made for the experiment. Furthermore, a small glass chamber was used to introduce solid carbon source, camphor. This small chamber facilitates controlled reaction of precursor with the substrate. Two separately controlled furnaces were used at the same time. One was for the precursor (furnace 1) and the other for placing the substrate (furnace 2). Argon and hydrogen with a ratio of 3:1 and purity of 99% were used to carry the precursor and react with the Cu placed in furnace 2. Introduction of the precursor to the substrate was controlled by a two-way carrier gas ($Ar+H_2$) insertion mechanism; one way was to carry $Ar+H_2$ to the substrate through the precursor chamber (F2) and the other was through the quartz tube (F1),as shown in Fig. 1.

Cleaning was performed by sonicating the Cu substrates for 5 min in acetone, then rinsed in methanol followed by isopropanol. The substrate was heated at 1000 °C for 60 min before deposition. Deposition was carried out at 1050 °C for 30 min in furnace 2. The precursor chamber was placed in the center of the furnace 1 and the temperature was set at 85–110 °C. The flow rate of $Ar+H_2$ was precisely controlled from 6 to 24 sccm inside the quartz tube (F1) and 3 sccm inside the precursor chamber (F2). Samples were taken out immediately after the deposition. As-grown samples were characterized by Field Emission Scanning Electron Microscopy (FESEM, JEOL JSM −7001FF), Raman Spectroscopy (green laser with excitation wavelength of 532 nm, JASCO NRS-1500W) and Raman mapping by NRS-3300 and Transmission Electron Microscopy (TEM) by JEM-2100F by JEOL.

3. Results

In the current approach, the intensity of nucleation of carbon was reduced on the Cu substrate and controlled growth was obtained by changing the carrier gas and carbon source insertion. This was accomplished by varying the temperature of furnace 1 in the range of 80–110 °C. Further control over the flow of precursor was obtained by controlling F_2 and F_1 (as shown in Fig. 1).

Fig. 2(a–c) shows FESEM images, demonstrating morphological structure of Cu foil. The sample was annealed at 1050 °C with gas flow of 3 sccm and 6 sccm for both F1 and F2 accordingly. The grain boundaries, location of the nanoparticles and wrinkles in the substrates are clearly visualized in these figures. Fig. 2(a) shows

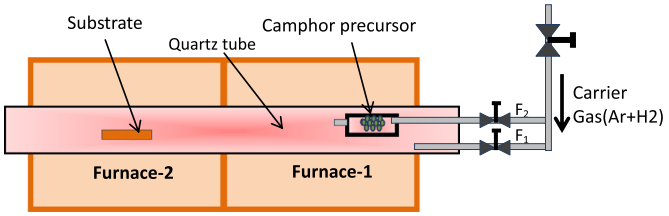

Fig. 1. Schematic of two furnace arrangement and two-fold gas insertion mechanism.

with an × 10,000 magnification that more than 50% of the captured area is white and the remaining area is black with some nanoscale white spots in the 40–100 nm range.

In the white area, the intensity of those white nanoparticles is much higher. To investigate the correlation of those nanoparticles with surface morphology, a spot (yellow rectangle in Fig. 2(a)) with a few nanoparticles is considered by FESEM, as shown in Fig. 2(b). The × 20,000 magnified image shows the NP are clustered near the wrinkles in the copper foil. Some grey and darker shades which are apparently graphene/graphite are to be found near those nanoparticle sites (red arrows). Areas near red arrow shows nanoparticles are densely situated which indicates that formation of those shaded area are influenced by the presence of NP near the wrinkles. To verify the impact of NP on shaded areas, image of × 30,000 magnification was taken (Fig. 2(c)) which shows existence of nanoparticle near the wrinkles on the surface. Furthermore, density of NP is high near graphene layers which validate preferential graphene/graphite growth near nanoparticles.

For further investigation of the nucleation of NP and graphitization on the surface, EDX analysis was performed, as shown in Fig. 3(a). Two areas on Cu surface were considered for the analysis: Yellow Square with no white nanoparticles (point 1) and Green Square with dense white particle (point 2). Within the Yellow Square, the measured weight percentage and atomic percentage of carbon are 0.60% and 1.03%, respectively. In contrast, a green square with few white spots is found to be more carbon rich. The weight percentage and atomic percentage of carbon at this spot are 1.27% and 8.15%, indicating a significant lower percentage of carbon at point 1 than point 2. Furthermore, amount of Cu is higher in yellow square compare to green one, as shown Table 1. Apart from carbon and copper, percentage of oxygen in point 1 is significantly lower than point 2, as shown in Table 1, indicating preferential growth of oxide nanoparticles of Cu. It is also observed that NP catalyses more carbon to be diffused and helps to form graphene or graphite indicated by shaded grey surrounding white NP. The optical image shows a clear contrast indicating difference for graphene sheets, as shown in Fig. 3(b). A Raman spectroscopic image near the black spot shows an intense G peak with significantly low intensity 2D peak which confirms the formation of sp^2 carbon with graphitic nature. The Raman spectroscopic image in the red circle also suggests carbonization (Fig. 3(c)) with the similar intensity of D, G and 2D peak, indicating a few layers of graphene. Comparing these findings with the EDX result, it can be deduced that the shaded structure on the optical image is mostly graphite flakes which reside near NP and the unshaded area represents amorphous carbon-rich areas where NP do not exist.

Fig. 4 shows the XRD pattern of the surface before and after graphene deposition. Several peaks are dominant at 38.14°, 43.56°, 44.37°, 50.62° and 64.7°. The peak at 44.37° and 50.62° correspond to metallic copper of Cu (111) and Cu (200) planes respectively. Other peaks represent oxide nanoparticles of Cu. Peak at 38.14° relates to CuO (200) whereas, peaks at 43.56° and 64.7° represent Cu_2O(200) and Cu_2O(220) plane respectively. It is obvious that the peak intensity of metallic copper, CuO and Cu_2O reduce after the deposition of graphene. Furthermore, the graphene/graphite peaks